**International Journal of Engineering and Information Systems (IJEAIS)**
**ISSN: 2643-640X**
**Vol. 5 Issue 2, February - 2021, Pages: 107-116**

# Investigation of the Performance of Model Predictive Control for Induction Motor Drives

**Ahmed G. Mahmoud A. Aziz[1], Yehia Sayed Mohammed[2], Hamdi Ali[3], Ahmed A. Zaki Diab[4*]**

[1,2,4]Dep. of Electrical Engineering, Faculty of Engineering, Mina University, Minia 61111, Egypt;
[1,3]Dep. of Electrical and Computer Engineering, El_Minia High Institute of Engineering and Technology, Minia 61111, Egypt.
[*]**Correspondence: Ahmed A. Zaki Diab, a.diab@mu.edu.eg, https://orcid.org/0000-0002-8598-9983**

***Abstract***—*The current work presents speed, torque and flux control of an induction motor (IM) drive, founded on model predictive control (MPC) .Via the MPC techniques, the motor electromagnetic torque and flux linkage are controlled as an internal loop. However, the speed is controlled as the external loop. The internal control loop is founded on finite control set FCS-MPC, and the external control founded on the torque PI controller. The performance of the MPC is tested with various conditions of the drive operation, and the outcomes approve the excellent steady-state and dynamic operation of the system in a wide range of speeds and with torque disturbance.*

**Keywords—**induction motor; Model Predictive Control; Finite Control Set

## 1. Introduction

The Direct Torque Control (DTC) method selects the calculated magnitude of stator flux and the calculated torque as the two control state variables. It utilizes a closed-loop feedback control assembly to make the flux and torque errors not exceed the hysteresis band (a predetermined band limit) [1-4]. The errors are estimated as the variance between the reference and the calculated value of the flux and torque. DTC requires the application of hysteresis band comparators as an alternative of flux and torque controllers. The DTC employs a pre-defined search table to choose the switching procedure based on the inverter mode. Merits of DTC strategy are concise as, rapid transient response, easy configuration and minimal parameter reliance [3-6]. However, the old DTC method has the disadvantages of significant-high torque and flux spikes. As probable substitute control plans, MPC is applied to the DTC to assuring the straight selection of the suitable switch states.

MPC employed to power electronics has two chief variations: Continuous Control Set MPC (CCS-MPC) [5], [6] and FCS-MPC [6]. The CCS-MPC estimations use the result of an adjusted drawback and a modulation phase produces a switch state of the converter stimulation. FCS-MPC utilizes the separate character of the power converter and a model of the load to resolve the adjustment problem comprehensively. FCS-MPC was utilized in many purposes, like conventional 3-phase 2-level inverters [8], [9].

Lately, MPC has gotten a high consideration in power electronics and motor drives because of the compensations of simple perception, fast-answer in addition to an excessive flexibility to include numerous restraints [10–12]. Several investigations have been performed on the correlated application of the MPC in power electronics and drives. Limited Control Set MPC (FCS-MPC), between MPC methods, is the exclusive one because of the discrete character of an inverter and giving the best solution for the on-line optimization challenge. Additionally, easy digital employment and guarantee of nonlinearities and restraints of MPC were additional characteristics of this algorithm [13-15].

The Predictive-Torque Control (PTC) method, utilizing FS-MPC in directly torque & flux controlling of an IM, was introduced in [16]. In PTC for an IM, a rule like the DTC is employed [1, 26]. The core attention of PTC is the estimate of torque and stator flux for every probable inverter switching modes. At that time a pre-defined cost-function estimates forecast values and lastly, a trajectory that has a minimum cost-function is elected. The system constrictions, numerous control objects and variables may be added to the cost-function simply. This plan doesn’t want Park transformation, exterior tuner, tuning technique of the controller’s components and internal current control loop. However, PTC wants a high-frequency sampling to achieve high-performance. The Implementation of PTC algorithm extends the period significantly, and this leads to the sampling of low-frequency and unsought influences on the functioning of the drive system.

Wang, Demonstrated the FS–MPC as a modern method. FS–MPC is more straight forward in the concept of design, it has a fast dynamic and good torque response; the experimental results verify that all strategies theoretical [17].

Shafiq Odhano, Stated that an MPC as a substitute to the linear controller-based Direct flux and current vector-control of IMs, a judgment among MPC and PI controller, was performed by experimentation. Simultaneously, the FCS-MPC results rich harmonic content in stator current that negatively impacts the drive presentation and efficiency. However, MPC has benefits over PI regulator in that the controller tuning is not essential with MPC [18].

Cristian Garcia, presented a cascaded construction for the control of an IM which is concerned utilizing the FCS-MPC. The control strategy has two loops, external and internal. The control external-loop is for speed. In contrast, the internal-loop controls the stator current. The experimental consequences illustrate that the planned strategy has a performance that is matching the classical control plans but that it is overshoot-free and gives an improved response time [19].

## 2. MATHEMATICAL MODEL OF THE IM

In the current reference framework, the stator voltage $v_s$ of IM consists of a stator resistance voltage decrease and the alteration rate of the stator flux-linkage. The IM stator voltage function (in stationary $(\alpha - \beta)$ reference frame) could be described as follows [1, 25]:

$$v_s = R_s i_s + p\, \Psi_s \tag{1}$$

Where,

$$v_s = [v_{s\alpha} \quad v_{s\beta}], \quad i_s = [i_{s\alpha} \quad i_{s\beta}] \text{ and } \quad \Psi_s = [\Psi_{s\alpha} \quad \Psi_{s\beta}]$$

The electromagnetic torque equation has the following expression:

$$T_e = 1.5\, n_p (i_{s\alpha}\, \Psi_{s\beta} - i_{s\beta} \Psi_{s\alpha}) \tag{2}$$

The dynamic mechanical system equation may be presented in the subsequent method:

$$T_e = T_L + Jp\, \omega_r + D\, \omega_r \tag{3}$$

The rotor angular speed is given as the time differentiation of the rotor position angle:

$$\omega_r = p\, \theta_r \tag{4}$$

Preserving the stator flux to be constant, the difference of the electromagnetic torque ($T_e$) depending on the path of the used voltage vector, such that:

$$T_e = \frac{P}{2} \frac{M}{L_r\, L_s - M^2} |\Psi_s||\Psi_r|\, sin\left(\dot{\delta}\, t\right) \tag{5}$$

where $\dot{\delta}$ is the angular speed of the stator flux-linkage relative to rotor flux-linkage. The equation of torque demonstrates that the torque could be controlled via controlling the relative speed among the stator and rotor fluxes at steady stator flux amplitude. As the electrical time-constant is significantly lower than the mechanical time-constant, the torque could be controlled via controlling the velocity of stator flux.

## 3. THE DYNAMIC MODEL OF THE IM

The IM dynamic model could be mentioned by the differential equations [25, 26]:

$$\frac{di_{\beta s}}{dt} = -\left(\frac{R_s}{L_s\delta} + \frac{R_r L_m^2}{L_s L_r^2 \delta}\right) i_{\beta s} + \frac{R_r L_m}{L_s L_r^2 \delta} \Psi_{\beta r} - \frac{L_m}{L_s L_r \delta} \omega_r \Psi_{\alpha r} + \frac{1}{L_s \delta} v_{\beta s} \tag{6}$$

$$\frac{di_{\alpha s}}{dt} = -\left(\frac{R_s}{L_s\delta} + \frac{R_r L_m^2}{L_s L_r^2 \delta}\right) i_{\alpha s} + \frac{R_r L_m}{L_s L_r^2 \delta}\, \Psi_{\alpha r} + \frac{L_m}{L_s L_r \delta} \omega_r \Psi_{\beta r} + \frac{1}{L_s \delta} v_{\alpha s} \tag{7}$$

$$\frac{d\Psi_{\beta r}}{dt} = \frac{R_r L_m}{L_r} i_{\beta s} - \frac{R_r}{L_r} \Psi_{\beta r} + \omega_r \Psi_{\alpha r} \tag{8}$$

$$\frac{d\Psi_{\alpha r}}{dt} = \frac{R_r L_m}{L_r} i_{\alpha s} - \frac{R_r}{L_r} \Psi_{\alpha r} - \omega_r \Psi_{\beta r} \tag{9}$$

$$\frac{d\omega_r}{dt} = \frac{1}{J}(T_e - T_l) - \frac{f_b}{J} \omega_r \tag{10}$$

where p is a differential operator; $R_s$, $R_r$ are the stator and rotor resistance, respectively; $\omega_r$ is the rotor speed, s is the slip, and P is the pole-pairs.

## 4. DERECT TORQUE CONTROL OF IM

The selection of the stator voltage vector regarding the difference among the reference flux & torque and their real values is the DTC basic principle [1-6]. To generate digital signals, the errors are fed over the separate hysteresis band matchers. The 3D look-up tables subsequently choose the suitable voltage vector to fulfill the flux & torque commands. The compensations of DTC strategy are briefed as a simple configuration, fast transient reply, and fewer parameter requirements [3-6].

The DTC is guaranteeing the straight selection of the optimal switch-modes, and so the stator voltage vector so as to retain the flux & torque errors does not exceed the hysteresis-band (a predetermined band limit) [1-3]. The errors were estimated by the variance among the reference and the estimated values of the flux & torque dissimilar to the FOC. The DTC needs the use of hysteresis band comparators in place of flux & torque controllers. The DTC utilizes a look-up table to choose the switching-process founded on the inverter states. The stator flux-linkage components can be getting it from the following equations:

$$\hat{\Psi}_{\alpha s} = \int (v_{\alpha s} - R_s\, i_{\alpha s})\, dt + \Psi_{\alpha s}(0) \tag{11}$$

$$\hat{\Psi}_{\beta s} = \int \left(v_{\beta s} - R_s\, i_{\beta s}\right) dt + \Psi_{\beta s}(0) \tag{12}$$

where $\Psi_{s\alpha}(0)$ and $\Psi_{s\beta}(0)$ are the primary-condition of stator flux parameters.

For the IM, the stator flux primary values are set to zero [1]. The stator flux value could be calculated as:

$$\left|\hat{\Psi}_s\right| = \sqrt{\hat{\Psi}_{\alpha s}{}^2 + \hat{\Psi}_{\beta s}{}^2} \tag{13}$$

The electromagnetic-torque could be calculated by stator current and calculated stator flux as:

$$T_e = \frac{3}{2}\, P\, (i_{\alpha s}\, \Psi_{\beta s} - i_{\beta s} \Psi_{\alpha s}) \tag{14}$$

If the time-period is appropriately short, ignoring the stator resistance voltage drop, the practical voltage space-vector gives a stator flux alteration having a similar path of the voltage space-vector. The value of stator flux space-vector was reserved stable by the application of the suitable voltage space-vectors. Simultaneously, the phase angle of the stator flux space-vector may be quickly altered by the application of voltage space-vectors, leads to a fast alteration of the torque-angle. Then the electromagnetic-torque could be quickly altered by altering the torque-angle in the needed path.

Briefly, the torque may be controlled by voltage space-vectors. For every part, two voltage vectors were chosen to raise or reduce the value of stator flux. A look-up table gives the switching-states to the control of height and direction of the stator flux. In this table, $\theta_s$ is the area number for stator flux-linkage, $H_\Psi$ is the hysteresis-controllers outputs for flux-linkage and $H_T$ is for torque. The block drawing of an IM drive with velocity control founded on DTC scheme is presented in Fig. 1. The stator currents & voltages are measured and converted into equivalent $\alpha - \beta$ values. The stator flux and electromagnetic-torque are assessed by measuring the current & voltage. Alternatively, the motor velocity is matched with the reference one to produce the torque-command. The torque & flux commands are matched with the equivalent calculated values and the errors are fed within the respective hysteresis-band comparators so as to produce a digital signal. A 3D look-up table at that time picks out the suitable voltage vector to fulfill the flux & torque commands. The controlling switching-states of the amplitude and stator flux direction are shown in a look-up table [5].

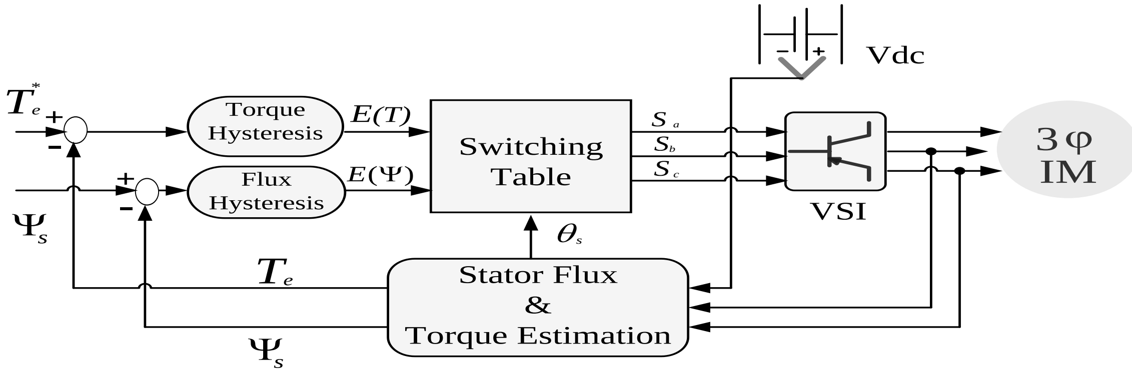


**Fig. 1.** *DTC scheme.*

## 5. Proposed MPC based IM drive

### 5.1 Basics of The MPC

The MPC is one of the best methods of control because of its merits of rapid dynamic reply, intuitive concept, the capability to handle many nonlinear limitations multivariable control, and so on. For IMs of high-performance frequently torque and stator flux are elected like a control variable. In conventional MPC, a cost-function concerning the torque & flux errors is outlined and assessed for every voltage vector and the one minimalizing the cost-function is elected like the best voltage vector [14].

In the MPC, the system model is taken into account so as to count the upcoming variables performance within a time frame (integer multiplication of the sample-period). These estimates are founded on a cost-function and subsequently reduces the cost-function is selected, finding, in this method, the upcoming control activities. Solitary the first value of the order is used, and the algorithm is considered each sample-time again. MPC has numerous compensations as the simple presence of nonlinearities and restrictions. This arrangement has limited uses in the power converter control and drives because of the high values of calculations required so as to resolve the regulation drawback online [24].

An additional method for implementing MPC in the power converters and drives was to utilize the benefit of the power converters discontinuous character. Although the power converters have limited switching states, the MPC optimization difficulty could be simplified and decreased to the estimate of system performance solitary for those probable switching-states. So, every estimate is employed to assess a cost-function (also identified as quality or decision function) and subsequently, the state with the smallest cost is elected and created. This method is identified as a FCS-MPC; also the probable control deeds (switching-states) are limited. This technique additionally identified as limited alphabet MPC or easily as predictive control, and it was effectively functional to a widespread-range of the power converter and drive uses [21].

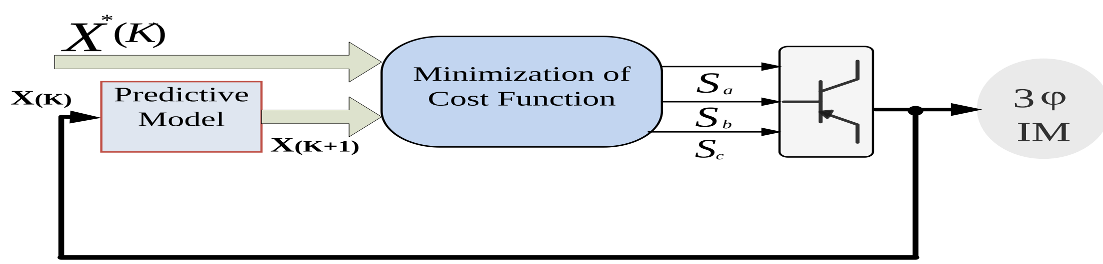


**Fig. 2.** *General MPC Scheme.*

### 5.2 The MPC scheme

MPC is one of the best control approaches owing to its qualities of obvious concept, multi-variable control, rapid dynamic response, capability to handle several nonlinear constraints, a model of the arrangement is measured so as to expect the upcoming performance of the variable quantity over a time frame, These calculations are assessed founded on a cost-function, and then, the arrangement that reduces the cost-function is selected, gaining, in this method, the upcoming control actions. Only the first order value is used, and the algorithm is intended once more every sampling-period.

A block drawing of the predictive control arrangement is introduced in Fig. 2. Quantities of several variables $x(k)$, as currents, voltages and velocity, were employed by the predictive-model to compute the upcoming controlled-variables values $x(k+1)$ for the complete probable voltage vectors. These calculations are assessed via the cost-function regarding the reference values $x^*(k)$. The voltage vector (or switching-state) that reduces the cost-function is elected and used within the following sampling-time. The subsequent paragraphs give several examples of the applications of the control scheme. Altogether the control arrangements were estimated via a cost-function g and a discrete-period model employed in calculation. It is revealed that the error of the current/torque/flux in an IM, the rapid power and the DC-link voltage are variables that could be controlled.

### 5.3 The PTC method

The PTC utilizes the basis like to DTC. In this arrangement, the best voltage vector is elected by approximation, calculation and cost-function optimizing technique [22]. An easy prognostic torque control arrangement is introduced in Fig. 3. In PTC technique, the stator & rotor fluxes at the current sampling-stage k are assessed. The stator & rotor fluxes estimate could be calculated by:

$$\hat{\bar{\varphi}}_s(k) = \hat{\bar{\varphi}}_s(k-1) + T_s\,\bar{v}_s(k) - R_s T_s \bar{i}_s(k) \tag{15}$$

$$\hat{\bar{\varphi}}_r(k) = \frac{L_r}{L_m}\hat{\bar{\varphi}}_s(k) + \bar{i}_s(k)\left(L_m - \frac{L_s L_s}{L_m}\right) \tag{16}$$

where $\hat{\bar{\varphi}}$ is the assessed value of $\bar{\varphi}$ and $T_s$ is the sampling-period.

## 6. Torque and Flux Prediction

A Guess of stator flux $\bar{\varphi}_s$ and electromagnetic-torque T for every voltage vectors of 2L-VSI necessary to be performed. The stator flux will be guessed:

$$\hat{\bar{\varphi}}_s^p(k+1) = \hat{\bar{\varphi}}_s(k) + T_s\,\bar{v}_s(k) - R_s T_s \bar{i}_s(k) \tag{17}$$

The torque calculation is connected to the calculated stator flux and current values; thus, the torque calculation function is:

$$T^p(k+1) = \frac{3}{2} p\, Im\left\{\hat{\bar{\varphi}}_s^p\,(k+1)\bar{i}_s^p(k+1)\right\} \tag{18}$$

It is essential to guess stator current for instant $k+1$. In this circumstance, the current calculation is,

$$\bar{i}_s^p(k+1) = \left(1+\frac{T_s}{\tau_\sigma}\right)\bar{i}_s(k) + \frac{T_s}{\tau_\sigma + T_s}\left\{\frac{1}{R_\sigma}\left[\left(\frac{k_r}{\tau_r} - k_r\, j\, \omega\right)\hat{\bar{\varphi}}_r(k) + \bar{v}_s(k)\right]\right\} \tag{19}$$

The stator flux was introduced in relations of the inverter voltages $\bar{v}_s(k)$, thus 7-various calculated stator flux and torque values are gotten. The values are assessed in a cost-function is chosen as the best vector. In the conventional PTC arrangement, the subsequent cost-function is employed :

$$g_h = \left|T^* - T^p(k+1)\right| + \lambda_\Psi\left|\varphi_s^* - \bar{\varphi}_s^p\,(k+1)\right| \tag{20}$$

where $\lambda_\Psi$ is the weighting factor that introduce the control objects rank.

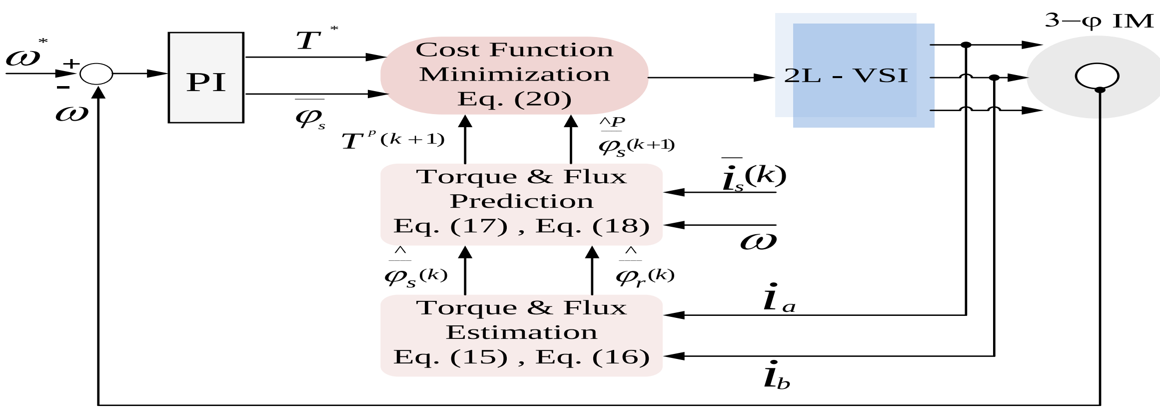


**Fig. 3.** *PTC scheme.*

## 7. CONTROL SCHEME BASED MPC

Recently, a lot of studies were performed on the MPC implementation in the drives and power electronics. The MPC methods that have been employed in Power Electronics were categorized into two core types [12, 14]: FCS-MPC and CCS-MPC. In the first set, a modulator produces the switching-states beginning from the predictive-controller continuous output. On the contrary, the FCS-MPC method uses the benefit of the switching-states fixed number of the power converter for resolving the regulation limitation. A disconnected model was employed to expect the system performance for each allowable actuation arrangement up to the prediction limit. The switching act that reduces a pre-defined cost-function is eventually designated to be used in the next sampling-period. The chief benefit of FCS-MPC was the straight use of the control action to the inverter, with no need of a modulation stage [23-24].

The PTC method, using FS-MPC in IM direct torque-flux control, is based on the torque and stator flux estimate for every possible inverter switching-states. A pre-defined cost-function assesses predicted values, and eventually, a vector by lessening the cost-function is elected. The system restrictions, some control items and variables can be easily added to the cost-function. This plan doesn't require Park transformation, external modulator, modification practice of the controller's parameters and the loop of internal current control [26].

Expensive DSP or FPGA hardware must be introduced to surmount the high computational problem of this algorithm. Furthermore, the limited amount of the inverter switching-states, laterally with the opportunity of using numerous successive switching-states, leads to variable switching-frequency. These two core drawbacks lead to difficulties of the PTC implementation in industrial systems [7].

Concerning the complex computational problem, it was proved that the number of permissible switching-states of an inverter has a high effect. So, multi-level inverter approaches are not extensively utilized with FS-PTC in industrial uses [9, 10].

## 8. RESULTS AND DISCUSSION

The IM drive Parameters are listed in Table 1. The IM drive based MPC has been tested under operation conditions using the proposed control scheme of fig. 3. The reference and actual values of torque/flux/speed are given in different cases in order to demonstrate the drive performance.

### 8.1 Case 1

Figure 4 displays the act of the drive system at forward and opposite velocity, the amplitude of stator flux with a stable value of (0.71 wb). And the timing sequence as following, At (t = 0 sec.) the motor is started, during (2 sec.) reference speed is increased linearly up to (10 rps), and kept constant for (2 sec.), at (t = 4 sec.) reference speed decreases linearly up to (-10 rps) and kept constant for (2 sec.), at (t = 8 sec.) the reference speed goes to (0 rps) in (2 sec.), the load-torque is kept constant at (10 Nm) during simulation period, from the consequences, a good dynamic act has been accomplished at the circumstance of changing speed in forward and reverse, and it may be noticed that the real electrical torque could follow the reference torque splendidly.

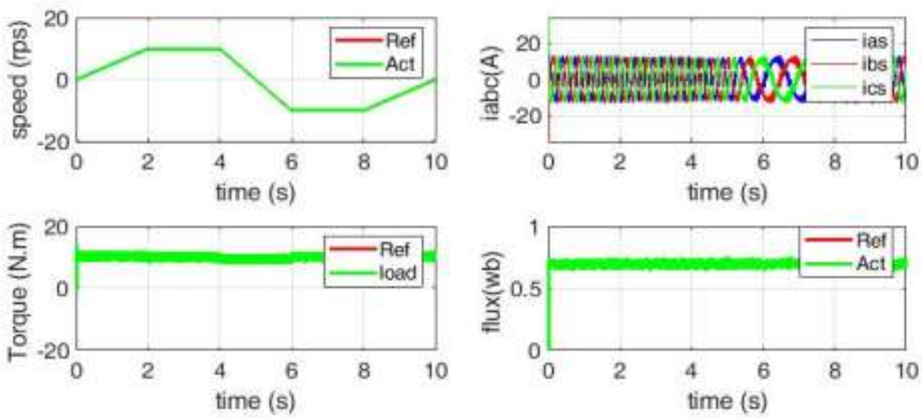


**Fig. 4.** *The performance of IM drive-based MPC for Case 1.*

**8.2** Case 2

Figure 5 shows the real velocity can track the reference velocity, the phase current is sinusoidal, and the amplitude of stator flux with a stable value of (0.71 wb). While the timing sequence as following, At (t = 0 sec.) the motor is started, during (2 sec.) reference speed is increased linearly up to (10 rps), and kept constant for two second, at (t = 4 sec.) reference speed decreases linearly up to (-10 rps) and kept constant for (2 sec.), at (t = 8 sec.) the reference speed goes to (0 rps) in (2 sec.), the load-torque is reserved steady at (18 Nm) during simulation period, from the consequences, an excellent dynamic act was accomplished at the circumstance of altering velocity in forward and opposite, and it could be noticed that the real electrical torque can follow the reference torque wonderfully.

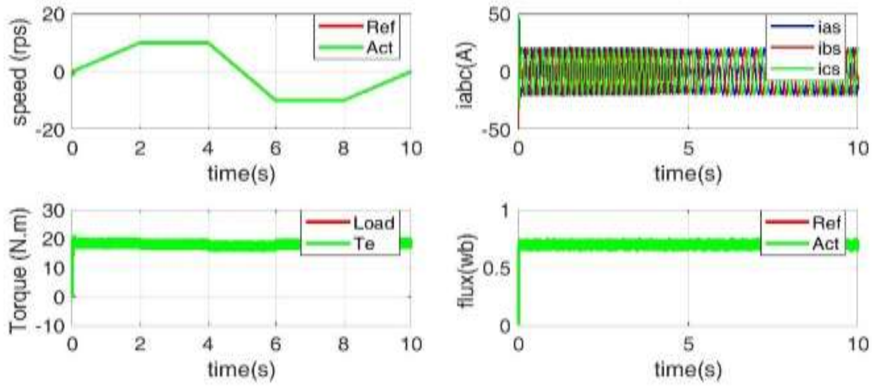


**Fig. 5.** *The performance of IM drive based MPC for Case 2.*

**8.3** Case 3

Figure 6 displays the act of the drive system at forward and opposite velocity, stator flux height with stable level of (0.71 wb). At (t = 0 sec.) the motor is started, during (2 sec.), reference speed is increased linearly up to (200 rps), and kept constant for (2 sec.), at (t = 4 sec.) reference speed decreases linearly up to (-200 rps) and kept constant for (2 sec.), at (t = 8 sec.) the reference speed goes to (0 rps) in (2 sec.), the load-torque is reserved steady at (10 Nm) within simulation period, from the consequences, a better dynamic act has been accomplished at the circumstance of changing speed in forward and reverse.

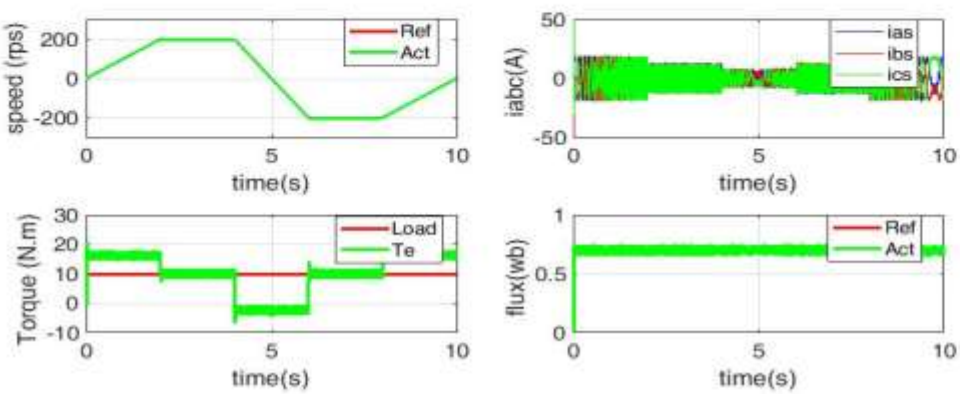


**Fig. 6.** *The performance of IM drive based MPC for Case 3.*

**8.4** Case 4

The consequences demonstrate the real velocity can track the reference speed, and the stator flux height with constant amount of (0.71 wb). And the timing sequence as following, At (t = 0 sec.) the motor is started, during (2 sec.) reference speed is increased linearly up to (200 rps), and kept constant for (2 sec.), at (t = 4 sec.) reference speed decreases linearly up to (-200 rps) and kept constant for (2 sec.), at (t = 8 sec.) the reference speed goes to (0 rps) in (2 sec.), the load-torque is kept constant at (13 Nm) during simulation period. The performance of such case of study has been shown in fig. 7.

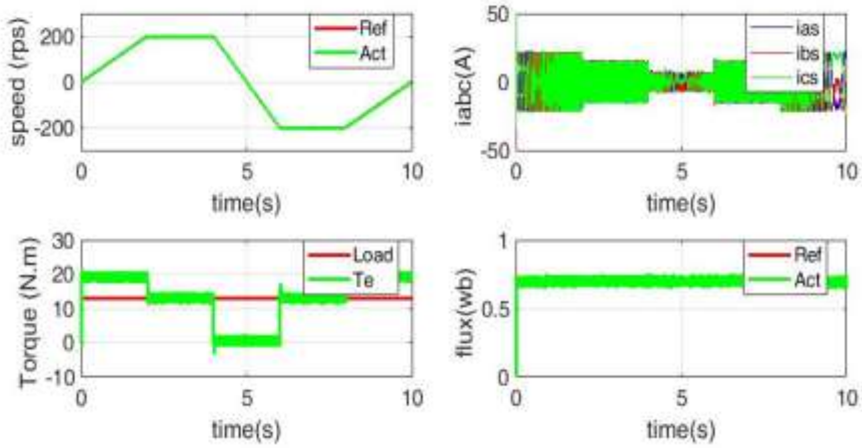


**Fig. 7.** *The performance of IM drive based MPC for Case 4.*

**8.5** Case 5

The results evidenced a good dynamic performance, quick recovering from load disturbance, the phase current is sinusoidal, And the timing sequence as following, A load-torque of (5 Nm ) is employed on the motor at starting, after (2 sec.) and is changed to (19 Nm) and return to (5 Nm) at (t = 4 sec.) and it kept at this value within the residual simulation interval, the reference speed remains constant at (10 rps) during simulation period, the results show the over-shoot and dip of the actual velocity. The performance of MPC based drive has been shown in fig. 8.

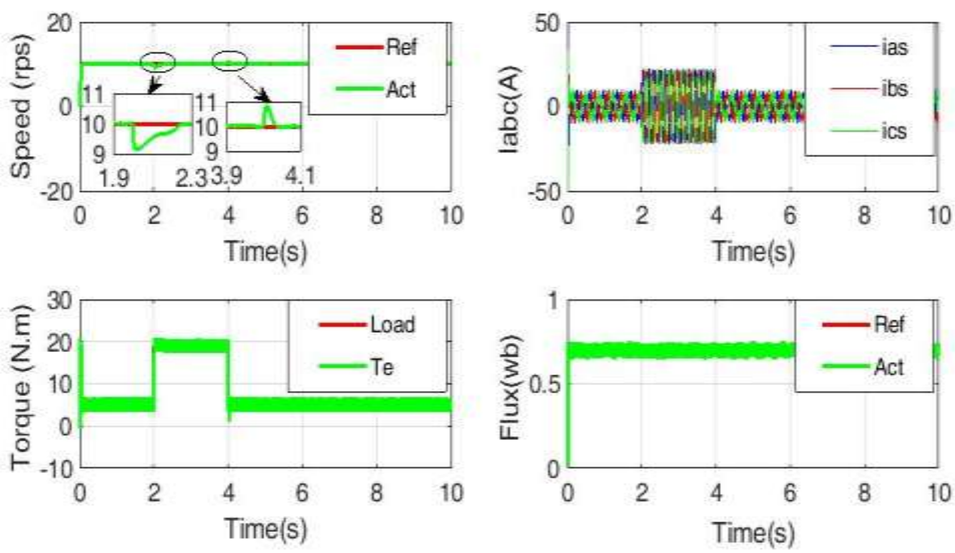


**Fig. 8.** *The performance of IM drive based MPC for Case 5.*

**Table 1.** IM Parameter.

| Symbol | Parameters | Values |
|---|---|---|
| $v_s$ | Rated voltage | 380 v |
| $n_p$ | No. pole pairs | 1 |
| f | Rated frequency | 50 Hz |
| $R_s$ | Stator resistance | 1.2 Ω |
| $R_r$ | Rotor resistance | 1 Ω |
| $L_s$ | Stator self-inductance | $175\ e^{-3}$ H |
| $L_r$ | Rotor self-inductance | $175\ e^{-3}$ H |
| $L_m$ | Magnetizing inductance | $170\ e^{-3}$ H |
| J | Moment of inertia | $0.062\ Kg.m^2$ |
| $\Psi_{sn}$ | Nominal stator flux | 0.71 Wb |
| $T_n$ | Nominal torque | 20 Nm |
| $R_m$ | Core-resistance | 2186 Ω |
| $T_s$ | Sampling-time | $4\ e^{-5}$ sec. |
| $K_p$ | Proportional gain | 3.016 |
| $K_i$ | Integrative gain | 0.141 |

## 9. Acknowledgment

A MPC of IM drives is introduced in the current work. The FS-MPC is a modern method for electrical drive systems which has fast dynamics and good torque response. The controller controlled straight the inverter switches to follow the IM velocity path, the controller does well in following the velocity path at low and high velocity. A cost-function involving of following error of stator flux and electromagnetic-torque to elect the finest voltage vector, the MPC controller has several compensations. In addition of being simple to construct and to be implemented, it has a very rapid reply, lesser ripples over currents and electromagnetic-torque relative to the traditional DTC approach. The simulation consequences display that the drive reply has several benefits: very rapid reply, robustness in contradiction of load variations and well following-up of velocity path at both low and high speeds.

## 10. References

**[1]** Takahashi and T. Noguchi, “A new quick-response and high-efficiency control strategy of an induction motor”, IEEE Trans. Ind. Electron.,vol. IA-22, no. 5, pp. 820–827, Sep. 1986.

**[2]** M. A. Rahman, and M. A. Hoque, “Sensorless direct torque control of induction motors used in electric vehicle”, IEEE Trans. On Energy Conversion, Vol. 18, No. 1, pp. 1-9, March 2003.

**[3]** Murat Barut, Seta Bogosyan and Metin Gokasan. “Speed sensorless direct torque control of IMs with rotor resistance estimation.”, Energy conversion and management, Vol. 46, pp. 335-349, 2005.

**[4]** Sultan H.M., Kuznetsov O.N., Diab A.A.Z., Site selection of large-scale grid-connected solar PV system in Egypt, (2018) Proceedings of the 2018 IEEE Conference of Russian Young Researchers in Electrical and Electronic Engineering, ElConRus 2018, 2018-January , pp. 813-818.

**[5]** Linder, Arne, Rahul Kanchan, Peter Stolze, and Ralph Kennel. "Model-based predictive control of electric drives.", Cuvillier, 2010.

**[6]** Mariethoz, Sebastien, Alexander Domahidi, and Manfred Morari. "High-bandwidth explicit model predictive control of electrical drives.", IEEE Transactions on Industry Applications 48, no. 6 (2012): 1980-1992.

**[7]** Ahmed A. Zaki Diab, Denis A. Kotin. and Vladimir V. Pankratov. "Speed control of sensorless induction motor drive based on model predictive control." In 2013 14th International Conference of Young Specialists on Micro/Nanotechnologies and Electron Devices, pp. 269-274. IEEE, 2013.

**[8]** Mossa, Mahmoud A., Hamdi Echeikh, Ahmed A. Zaki Diab and Nguyen Vu Quynh. "Effective Direct Power Control for a Sensor-Less Doubly Fed Induction Generator with a Losses Minimization Criterion." ,Electronics 9, no. 8 (2020): 1269.

**[9]** Mohamed I.S., Rovetta S., Do T.D., Dragicevic T., Diab A.A.Z., A neural-network-based model predictive control of three-phase inverter with an output LC Filter, (2019) IEEE Access, 7 , art. no. 8819887 , pp. 124737-124749.

**[10]** Y. Zhang and C. Qu. "Model predictive direct power control of PWM rectifiers under unbalanced network conditions.” IEEE Trans. Ind. Electron., vol. 62, no. 7, pp. 4011–4022, 2015.

**[11]** S. Vazquez, J. I. Leon, L. G. Franquelo, J. Rodriguez, H. A. Young, A. Marquez, and P. Zanchetta, "Model predictive control: A review of its applications in power electronics.", IEEE Ind. Electron. Mag., vol. 8, no. 1, pp. 16–31, March 2014.

**[12]** Y. Zhang, Y. Peng, and H. Yang, "Performance improvement of two vectors-based model predictive control of PWM rectifier.", IEEE Trans. Power Electron., vol. 31, no. 8, pp. 6016–6030, 2016.

**[13]** P. Cortes, M. P. Kazmierkowski, R. M. Kennel, D. E. Quevedo, and J. Rodriguez, "Predictive control in power electronics and drives.", IEEE Trans. Ind. Electron., vol. 55, DOI 10.1109/TIE.2008.2007480, no. 12, pp. 4312–4324, Dec. 2008.

**[14]** S. Kouro, P. Cortes, R. Vargas, U. Ammann, and J. Rodriguez, "Model predictive control-a simple and powerful method to control power converters.", IEEE Trans. Ind. Electron., vol. 56, DOI 10.1109/IPEMC.2009.5289335, no. 6, pp. 1826–1838, Jun. 2009.

**[15]** J. Rodriguez, M. P. Kazmierkowski, J. R. Espinoza, P. Zanchetta, H. Abu-Rub, H. A. Young, and C. A. Rojas, "State of the art of finite control set model predictive control in power electronics.", IEEE Trans.on Ind. Informatics, vol. 9, DOI 10.1109/TII.2012.2221469, no. 2, pp. 1003–1016, May 2013.

**[16]** H. Miranda, P. Cortes, J. I. Yuz, and J. Rodriguez, "Predictive torque control of induction machines based on state-space models.", IEEE Trans. Ind. Electron., vol. 56, DOI 10.1109/TIE.2009.2014904, no. 6, pp. 1916–1924, 2009.

**[17]** Fengxiang Wang, Zhenbin Zhang*, Xuezhu Mei, José Rodriguez and Ralph Kennel, " Advanced Control Strategies of Induction Machine: Field Oriented Control, Direct Torque Control and Model Predictive Control .", Energies 2018.

**[18]** Shafiq Odhano, Radu Bojoi, Andrea Formentini, Pericle Zanchetta and Alberto Tenconi, "Direct flux and current vector control for induction motor drives using model predictive control theory.", IET Electr. Power, Vol. 11 Iss. 8, pp. 1483-1491, Appl., 2017.

**[19]** Cristian Garcia, Jose Rodriguez, Cesar Silva, Christian Rojas, Pericle Zanchetta, and Haitham Abu-Rub, "Full Predictive Cascaded Speed and Current Control of an Induction Machine " IEEE TRANSACTIONS ON ENERGY CONVERSION, VOL. 31, NO. 3, SEPTEMBER 2016.

**[20]** Ahmed A. Zaki Diab. "Implementation of a novel full-order observer for speed sensorless vector control of induction motor drives." Electrical Engineering 99, no. 3 (2017): 907-921.

**[21]** R. Vargas, U. Ammann, J. Rodriguez, J. Pontt, "Predictive Strategy to Reduce Common-Mode Voltages on Power Converters", in Power Electronics Specialists Conference, PESC 2008, June 2008.

**[22]** J. Rodriguez and P. Cortes, "Predictive Control of Power Converters and Electrical Drives.", John Wiley & Sons, 2012.

**[23]** Ahmed A. Zaki Diab, D. A. Kotin, V. N. Anosov, and V. V. Pankratov. "A comparative study of speed control based on MPC and PI-controller for Indirect Field oriented control of induction motor drive." In 2014 12th International Conference on Actual Problems of Electronics Instrument Engineering (APEIE), pp. 728-732. IEEE, 2014.

**[24]** Ahmed A. Zaki Diab, V. V. Vdovin, D. A. Kotin, V. N. Anosov, and V. V. Pankratov. "Cascade model predictive vector control of induction motor drive." In 2014 12th International Conference on Actual Problems of Electronics Instrument Engineering (APEIE), pp. 669-674. IEEE, 2014.

**[25]** A. G. M. A. Aziz, A. A. Z. Diab, and M. A. E. Sattar, "Speed sensorless vector controlled induction motor drive based stator and rotor resistances estimation taking core losses into account," in 2017 Nineteenth International Middle East Power Systems Conference (MEPCON), 2017, pp. 1059-1068.

**[26]** A. G. M. A. Aziz, H. Rez, and A. A. Z. Diab, "Robust Sensorless Model-Predictive Torque Flux Control for High-Performance Induction Motor Drives," Mathematics, vol. 9, no. 4, 2021.